Low-Order Models for Catalyst Particles: A Dynamic Effectiveness Factor Approach

José Álvarez-Ramírez, Francisco J. Valdés-Parada, and J. Alberto Ochoa-Tapia
División de Ciencias Básicas e Ingeniería, Universidad Autónoma Metropolitana–Iztapalapa, Mexico, D.F., Mexico

DOI 10.1002/aic.10593
Published online August 31, 2005 in Wiley InterScience (www.interscience.wiley.com).

Models for heterogeneous reactors are composed of distributed parameter ordinary and partial differential equations to describe balances both for a fluid and a catalyst particle. For steady-state conditions, the effectiveness factor (EF) approach has been primarily used to reduce the model dimensionality, which yields an important computational effort during reactor design stages. The idea behind EF is to express the reaction rate in a catalyst particle by its rate under surface/bulk conditions multiplied by the EF. As a consequence, only few arithmetic operations to obtain the catalyst particle total reaction rate have to be made, avoiding in this form repeated solutions of the more sophisticated distributed parameter model. The aim of this paper is to extend the EF approach to obtain a simple model for the dynamics of the catalyst particle total reaction rate. As a preliminary step, a Laplace domain approach is used to introduce a dynamic EF (DEF) concept as a linear operator that transforms reaction rate signals from surface/bulk to catalyst particle conditions. It is shown that the DEF becomes the transfer function of a model governing the dynamics of the catalyst particle reaction rate. However, the resulting transfer function is infinite-dimensional. This implies that, contrary to the steady-state case, an exact simple modeling of the reaction rate dynamics is not possible. An approach to obtain low-order models, based on an approximate model matching, is proposed. For a first-order model, the time constant is computed for common particle geometries showing its dependency with the Thiele modulus. In fact, the results show that the (dominant) time constant is a decreasing function of the Thiele modulus. In this form, the faster the chemical reaction dynamics, the faster the reaction–diffusion catalyst particle dynamics. © 2005 American Institute of Chemical Engineers *AIChE J,* 51: 3219–3230, 2005

Keywords: catalyst particle, reaction–diffusion, low-order model, approximate model matching

Introduction

Dynamic models for heterogeneous reactors are composed of distributed parameter, ordinary, and partial differential equations to describe balances both for a fluid and a disperse phase composed by catalyst particles. Simple models for the fluid can correspond to continuous stirred tank assumptions, which yield coupled ordinary differential and algebraic equations. Given that intraparticle resistance to mass transfer becomes significant for catalyst particles, mass and energy balances can lead to distributed parameter differential equations to describe the concentration distribution into the catalyst particle. The fluid and the catalyst particle models are coupled through a mass-transfer flux on the particle surface, which depends on fluid conditions.

J. Álvarez-Ramírez is also affiliated with Programa de Investigación en Matemáticas Aplicadas y Computación, Instituto Mexicano del Petróleo.
Correspondence concerning this article should be addressed to J. Álvarez-Ramírez at jjar@xanum.uam.mx.

The design and analysis of heterogeneous reactors may involve repeated solutions of the model. For instance, within an optimization-based design methodology, the reactor model solution is required at each optimization trial. On the other hand, on-line reactor dynamic, or even steady-state, simulation would involve solving the reactor model for each simulation step. Accurate numerical solution of distributed parameter models, as in the catalyst particle case, can be made with standard finite-element and finite-difference methods. However, such methods lead, in general, to a large set of algebraic and differential equations. Under this situation, the computational burden involved in repeated reactor model solutions can be excessive or even prohibitive. Given its parameter distributed nature, in general, the largest numerical burden is associated with the catalyst particle model. This practical problem constitutes an incentive to find approximate dynamic models for heterogeneous reactors, specifically for catalyst particles. Indeed, this is the aim of the paper.

For steady-state conditions, the effectiveness factor (EF) approach has been largely used to reduce the model dimensionality.[1] The idea is to express the reaction rate in a catalyst particle by the reaction rate under surface/bulk conditions multiplied by the EF. As a consequence, only few arithmetic operations are required to obtain the catalyst particle reaction rate, avoiding in this form repeated solutions of the high-dimensional distributed parameter model. Few studies have focused on the issue of approximate methods for catalyst particles under dynamic conditions.[2-4] The proposal is to approximate the dynamic distributed parameter by a single initial-value differential equation describing the dynamics of the average particle concentration. The low-dimensional model has been derived as a long-time approximation and its accuracy increases for longer times.[4] A criticism to this approximation approach is that low-order models are oriented to describe average concentration dynamics, which are rarely of interest in most practical reactor design and simulation situations. Instead, variables such as the reaction rate provided by the catalyst particle are more useful to evaluate reactor performance. The attractiveness of the EF approach relies on the fact that it leads directly to the catalyst particle reaction rate as a function of bulk/surface conditions. In this way, reactor models are readily simplified by incorporating the particle reaction rate as a pseudo-reaction rate in the fluid mass balance. Unfortunately, an extension of the EF idea for dynamic conditions is not yet available.

The aim of this paper is to twofold:

(1) To extend the EF approach to dynamic conditions. To the best of our knowledge, a dynamic EF concept has not been reported previously in the open literature.

(2) To obtain a simple model for the dynamics of the reaction rate for a catalyst particle. To this end, we constrain ourselves to the linear case as a prerequisite to address the more interesting nonlinear case. In principle, this latter case can be addressed following similar ideas as those reported by Szukiewicz.[4]

In a first step, a Laplace domain approach is used to introduce a dynamic EF (DEF) concept as a linear operator that transforms reaction rate signals from surface/bulk to catalyst particle conditions. Similar to feedback control theory for hyperbolic and parabolic partial differential equations (PDEs),[5,6] what is done to compute the DEF is to formulate an output for linear parabolic reaction–diffusion equations, which is the spatial integral averaging of the dynamic reaction rate. In this form, it is shown that the DEF becomes the transfer function of a model governing the dynamics of the catalyst particle reaction rate. However, the resulting transfer function is *infinite*-dimensional. This implies that, contrary to the steady-state case, an exact simple (such as finite-dimensional) modeling of the reaction rate dynamics is not possible. To overcome this problem, an approach to obtain low-order models based on an approximate model matching is proposed. For a first-order model, the time constant is computed showing its dependency with the Thiele modulus. In fact, the results show that the (dominant) time constant is a decreasing function of the Thiele modulus. In this form, the faster the chemical reaction dynamics, the faster the reaction–diffusion catalyst particle dynamics. Numerical simulations are used to illustrate our findings.

Dynamic Effectiveness Factor

In this section, a DEF concept that extends the classical one based on nondynamic conditions is introduced. To this end, similar to the case of the dynamic permeability concept,[7] the catalyst particle dynamics will be represented in the Laplace/Fourier domain. Because we are concerned with fundamental concepts rather than with EF computations for general cases, analytic solutions for the reaction–diffusion process will be used. In this way, the concepts will be based on simple isothermic reaction–diffusion processes leading to linear differential equations.

Classical EF concept

As mentioned earlier, the classical EF concept pertains to nondynamic operating conditions. To recall the classical EF concept, consider an isothermic catalyst particle where a single first-order chemical reaction is taking place. In a general geometry, by assuming constant diffusivity D and a Fickian diffusion mechanism $\mathbf{J} = -D\nabla c$, the nondynamic process can be modeled as follows (throughout, overbars denote nondynamic conditions):

$$D\Delta\bar{c} - k\bar{c} = 0 \tag{1}$$

where $x \in \mathbb{R}^3$ is the system coordinates vector, $\bar{c}$ is the nondynamic reactive concentration, k is the reaction constant, and

$$\Delta = \frac{\partial^2}{\partial x_1^2} + \frac{\partial^2}{\partial x_2^2} + \frac{\partial^2}{\partial x_3^2}$$

The domain $D \subset \mathbb{R}^3$ of the catalyst particle is assumed to be simply connected. The boundary conditions for Eq. 1 are given by

$$\begin{aligned} &\bar{c}(x) = \bar{c}_b && \text{for all } x \in \partial D \\ &\bar{c}(x) \text{ is finite} && \text{for all } x \in D \end{aligned} \tag{2}$$

where $\bar{c}_b$ is a constant boundary concentration and ∂D denotes the boundary of the domain D. The linear Eq. 1 has a unique solution $\bar{c}(x)$ satisfying the boundary conditions of Eq. 2 [that

is, $\bar{c}(x) = \bar{c}_b$ for all $x \in \partial D$]. The EF expresses the reaction rate in a catalyst particle by the rate under surface/bulk conditions.[1] That is, the classical nondynamic EF (denoted by $\bar{\eta}$) is defined as follows:

$$\bar{\eta} \overset{def}{=} \frac{\int_D k\bar{c}dV}{\int_D k\bar{c}_b dV} \tag{3}$$

where $dV = dx_1 dx_2 dx_3$ is a generalized volume differential. Analytic solutions of Eqs. 1 and 2 can be obtained for simple geometries, and the EF expression can be computed by integration of the solution $\bar{c}(x)$ according to Eq. 3. Let

$$\Phi \overset{def}{=} \sqrt{\frac{kL^2}{D}} \tag{4}$$

be the Thiele modulus, where L is a characteristic thickness depending on the geometry. In fact, L is the slab length for rectangular geometry and L is the cylinder and sphere radius for cylindrical and spherical geometries, respectively. For common particle geometries analytical expressions are known in advance. In fact,

$$\bar{\eta}(\Phi) = \begin{cases} \dfrac{\tanh(\Phi)}{\Phi} & \text{for rectangular geometry} \\ \dfrac{2I_1(\Phi)}{\Phi I_0(\Phi)} & \text{for cylindrical geometry} \\ 3\left[\dfrac{1}{\Phi \tanh(\Phi)} - \dfrac{1}{\Phi^2}\right] & \text{for spherical geometry} \end{cases} \tag{5}$$

where I_1 and I_0 are the first- and zeroth-order modified Bessel functions of the first kind, respectively.

The importance of the EF to obtain a reduced-order model relies on the fact that it depends only on reaction and diffusion parameters by the Thiele modulus Φ, and not on the bulk/surface conditions. This means that the EF is invariant under perturbations of the bulk/surface fluid conditions. This property is exploited to obtain a useful reduced catalyst particle model. In principle, to compute the total reaction rate $\int_D k\bar{c}dV$ provided by the catalyst particle, one should solve the boundary-value problem of Eqs. 1 and 2. Standard efficient finite-element or finite-differences numerical methods can be used to this end. However, if such a computation has to be made iteratively, as in optimization-based designs, an excessive and sometimes prohibitive computational burden could be introduced. A reduced-order model is obtained from the EF concept as follows. Let

$$\bar{R} \overset{def}{=} \int_D k\bar{c}(x)dV$$

and

$$\bar{R}_b \overset{def}{=} \int_D k\bar{c}_b dV$$

be the reaction rate for particle and surface/bulk conditions, respectively. From Eq. 3, because $\bar{R}_b = Vk\bar{c}_b$, one obtains the relationship $\bar{R} = \bar{\eta}Vk\bar{c}_b$. In this way, the effects of changes in the fluid conditions, reflected in changes of $\bar{c}_b$, can be easily estimated, leading to a significant reduction of the computational effort during extensive reactor simulations.

Extending the effectiveness factor concept for dynamic conditions

An extension of the classical EF concept to dynamic conditions should retain the property of relating reaction rates from bulk/surface to particle conditions. Indeed, this property makes possible the reduction of the complexity of the catalyst particle model. To this end, we will interpret the EF as a scaling factor between two reaction functions. To do this we proceed as follows. It has been shown that $\bar{R} = \bar{\eta}\bar{R}_b$. The EF $\bar{\eta}$ can be seen as a steady-state operation that transforms reaction rate values at boundary conditions $\bar{R}_b$ into reaction rate values at catalyst particle reaction–diffusion conditions $\bar{R}$; that is,

$$\bar{\eta} : \bar{R}_b \rightarrow \bar{R} \tag{6}$$

An extension of the EF concept to dynamic conditions should retain the following salient characteristics:

(1) It should be a linear transformation between *dynamic* reaction rate functions at boundary conditions and *dynamic* reaction rate functions at catalyst particle (reaction–diffusion) conditions.

(2) When a dynamic EF is seen as an operator between such reaction rate functions, it should converge uniformly to the steady-state operator $\bar{\eta}$.

To introduce the DEF concept as a linear transformation between dynamic reaction rate functions, we resort to Laplace domain methods. Recall that if $f(x, t)$ is a time function, its Laplace transform $F(x, s) = \mathcal{L}[f(x, t)]$ is given by $F(x, s) = \int_0^\infty e^{-st} f(x, t)dt$, where s denotes the Laplace variable. If $c_b(t)$ is a dynamic boundary condition, its Laplace transform is $C_b(s) = \mathcal{L}[c_b(t)]$ and the corresponding dynamic reaction rate at boundary condition is $R_b(s) = VkC_b(s)$. The dynamic reaction rate at particle conditions $R(s)$ is computed as

$$R(s) = \int_D kC(x, s)dV \tag{7}$$

where $C(x, s)$ is the solution of the dynamic boundary-value problem (notice that sc is the Laplace transform of $\partial c/\partial t$):

$$D\Delta C - kC = sC \tag{8}$$

with boundary conditions

$$\begin{aligned} C(x, s) &= C_b(s) && \text{for all } x \in \partial D \\ C(x, s) &\text{ is finite} && \text{for all } x \in D \end{aligned} \tag{9}$$

Similar to the steady-state EF concept, we define the DEF as follows:

The DEF is a linear operator $\eta(s)$ that transforms dynamic total reaction rates at boundary conditions $R_b(s)$ into dynamic reaction rates at particle conditions $R(s)$.

That is, the DEF is defined as the transformation

$$\eta(s) : R_b(s) \rightarrow R(s) \tag{10}$$

In other words, the DEF is a linear operator satisfying the relationship

$$R(s) = \eta(s) R_b(s)$$

It is asked that $\eta(s) \rightarrow \bar{\eta}$ as $s \rightarrow 0$ (that is, steady-state conditions). By serving as the functional factor, the DEF should give some information on the effectiveness of a single catalyst particle when it is subjected to external perturbations in the surface/bulk conditions.

It should be remarked that the definition of the DEF as a linear dynamic operator between input $[R_b(s)]$ and output $[R(s)]$ signals is motivated by control theory concepts. Specifically, similar to the approach by Christofides and Daoutidis,[5,6] the signal $R(s)$ is an output of the linear parabolic PDE given by Eqs. 8 and 9. The computation of the DEF is equivalent to the computation of the transfer function between the input $R_b(s)$ and the output $R(s)$. In this way, as $\eta(s) \rightarrow \bar{\eta}$ when $s \rightarrow 0$ is required that $\bar{\eta}$ would correspond to the steady-state gain.

Computation of the DEF

In principle, to compute the DEF $\eta(\omega)$, one should find the solution $C(x, s)$ of the boundary-value problem (Eqs. 8 and 9) and use it to calculate $R(s)$ by the integral in Eq. 7. An expression for the DEF can be easily obtained from the nondynamic EF expressions (see, for instance, Eq. 5) by noticing that Eq. 8 can be written as

$$D\Delta C - \kappa(s)C = 0 \tag{11}$$

where $\kappa(s) = k + s$ can be interpreted as a dynamic reaction rate constant. By considering the boundary condition Eq. 9, Eq. 11 can be solved in a similar way as the nondynamic case (Eqs. 1 and 2). To this end, let us introduce the dynamic Thiele modulus

$$\Psi(s) \overset{def}{=} \sqrt{\frac{\kappa(s) L^2}{D}} \tag{12}$$

Thus, if $\bar{\eta} = \phi(\Phi)$ is an expression for the nondynamic EF, an expression for the DEF is obtained by a formal substitution $\Phi \leftrightarrow \Psi(\omega)$. That is, the DEF is obtained as

$$\eta(s) = \phi[\Psi(s)] \tag{13}$$

Because $\Psi(0) \rightarrow \Phi$, one obtains the desired convergence $\eta(0) = \bar{\eta}$ to nondynamic conditions.

The DEF can be expressed in terms of a normalized frequency as follows. Let

$$\omega_d = D/L^2$$

be the diffusion characteristic frequency. Introduce the normalized Laplace variable as (recall that s has frequency units)

$$s_n = \frac{s}{\omega_d} \tag{14}$$

In the time domain, the Eq. 14 normalization is equivalent to normalizing the time variable as $t\omega_d$. In fact, $t_d = \omega_d^{-1}$ can be interpreted as a characteristic diffusion timescale. For $\kappa(s) = k + s$ the dynamic Thiele modulus can be written as

$$\Psi(s_n) = \sqrt{\Phi^2 + s_n} \tag{15}$$

In this way, in terms of normalized variables, the DEF expressions for common geometries are the following:

$$\eta(s_n, \Phi) = \begin{cases} \dfrac{\tanh[\Psi(s_n)]}{\Psi(s_n)} & \text{for rectangular geometry} \\ \dfrac{2I_1[\Psi(s_n)]}{\Psi(s_n) I_0[\Psi(s_n)]} & \text{for cylindrical geometry} \\ 3\left[\dfrac{1}{\Psi(s_n)\tanh[\Psi(s_n)]} - \dfrac{1}{\Psi(s_n)^2}\right] & \text{for spherical geometry} \end{cases} \tag{16}$$

For convenience, the dependency of the DEF has been made explicit. In this way, $\eta(s_n, \Phi)$ can be seen as a family of linear operators parameterized by the classical Thiele modulus Φ.

Frequency response of DEF

For convenience the discussion throughout will be made in terms of the normalized variable s_n. For each Thiele modulus Φ, the DEF $\eta(s_n, \Phi)$ is a linear operator acting on reaction rate signals $R_b(s)$. Some salient characteristics of $\eta(s_n, \Phi)$ can be obtained by studying its frequency response in the Fourier domain. This is done by making the formal substitution $s \leftrightarrow i\omega$ ($s_n \leftrightarrow i\omega_n$), where ω is the frequency and $i = \sqrt{-1}$. For simplicity in presentation, computations are made only for rectangular geometry. Similar results are obtained for cylindrical and spherical geometries. Figures 1 and 2 show, respectively, the Nyquist plot $\mathrm{Re}[\eta(\omega_n)]$ vs. $\mathrm{Im}[\eta(\omega_n)]$ and the magnitude Bode plot $|\eta(\omega_n, \Phi)|$, for three different values of the Thiele modulus Φ. For comparison, the limiting case $\Phi = 0$ corresponding to a reaction-free process is also included. The following salient features are observed:

- For each Thiele modulus Φ, the Bode plot displayed in Figure 2 shows that the DEF magnitude $|\eta(\omega_n, \Phi)|$ is a monotonous decreasing function of the frequency ω_n. This means that the best reaction rate performance of a catalyst particle is found at nondynamic conditions. That is, the largest reaction rate $R_T(\omega_n)$ is obtained when the reaction–diffusion process is operated at steady-state conditions. Dynamic pertur-

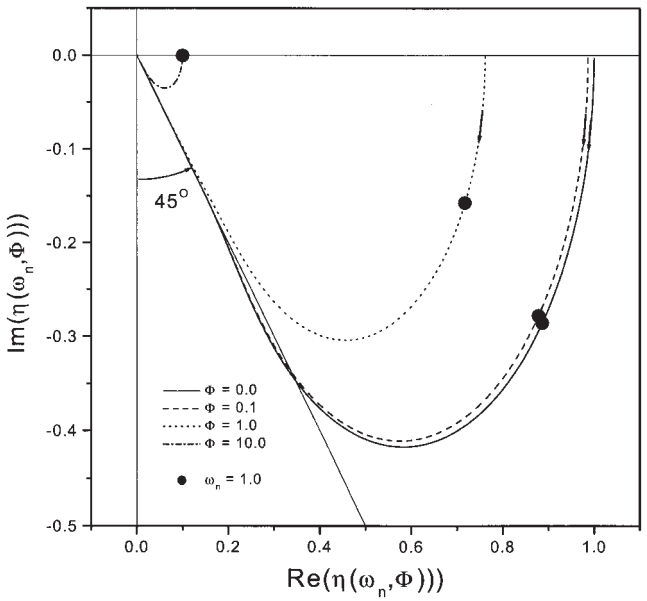

Figure 1. Nyquist plot for four different values of the Thiele modulus Φ.

Observe the high frequency convergence of the Fickian diffusion behavior $\eta(\omega_n, \Phi) \approx 1/\sqrt{i\omega_n}$.

bations will deteriorate the performance of the catalyst particle. This is an incentive to introduce control actions aimed at reducing dynamic perturbation effects on the system performance.

• For nondynamic conditions one has that $\bar{\eta}(\Phi_1) < \bar{\eta}(\Phi_2)$ for $\Phi_1 > \Phi_2$. That is, the nondynamic EF is a decreasing function of the classical Thiele modulus Φ. For each frequency ω_n, this property is maintained for the magnitude of the dynamic effectiveness factor $\eta(\omega_n, \Phi)$. In fact, Figure 2 shows that, as expected, $|\eta(\omega_n, \Phi_1)| < |\eta(\omega_n, \Phi_2)|$ for $\Phi_1 > \Phi_2$ and all ω_n. As a consequence, the DEF for the reaction-free case $\Phi = 0$ becomes an upper bound for the DEF $\eta(\omega_n, \Phi)$. That is, the largest DEF is obtained for reaction-free conditions. The Nyquist plot in Figure 1 shows that the curve $\Phi = 0$ surrounds the curves for $\Phi > 0$.

• Recall that the diffusion characteristic frequency ω_d has been used to normalize the frequency variable. In this way, $\omega_n = 1$ corresponds to $\omega = \omega_d$. Figure 2 shows that the DEF magnitude $|\eta(\omega_n, \Phi)| \approx \bar{\eta}(\Phi)$ for $\omega_n < 1$. That is, dynamic perturbations with frequencies lower than the diffusion characteristic frequency ω_d do not have a significant effect on the performance of a catalyst particle. As a consequence, the Nyquist plot of $\eta(\omega_n, \Phi)$ approaches the unit circle behavior for $\omega_n < 1$. This is illustrated in Figure 1 where the point corresponding to $\omega_n = 1$ has been marked. From the physical perspective, the behavior $|\eta(\omega_n, \Phi)| \approx \bar{\eta}(\Phi)$ for $\omega_n < 1$ can be explained by the fact that, because surface concentration fluctuations with $\omega < \omega_d$ are relatively slow compared with diffusion dynamics, the reactant supply into the catalyst particle bulk is not decreased. This allows the reaction–diffusion process to perform similarly to steady-state conditions. As previously observed by Christofides and Daoutidis,[5,6] when working with Galerkin approximation techniques, this suggests that the dynamics of the reaction–diffusion system are dominated by a few slow modes that can capture, to some degree, the dominant asymptotic spatiotemporal behavior of the overall reaction rate $R(s)$.

• For $\omega_d > 1$, the magnitude $|\eta(\omega_n, \Phi)|$ goes through a fast roll-down behavior to achieve values close to zero at high frequencies. This behavior is reflected in the Nyquist plot (Figure 1) as a fast convergence of the curve $\eta(\omega_n, \Phi)$ to the origin. The drastic deterioration of the catalyst particle performance when the perturbation frequency is increased beyond the diffusion characteristic frequency ω_d is attributed to a reduction in the effective usage of the particle space. In fact, when the frequency of the perturbation is large, $|\eta(\omega_N, \Phi)| \ll 1$ because reactants cannot penetrate the particles during one perturbation period. At high frequencies, the catalyst particle appears as a semi-infinite particle because of the limited penetration of the diffusion wave. In this form, for high-frequency perturbations the DEF is close to zero because a significant space of the catalyst particle is unused.

• For high frequencies, Figure 1 shows that the Nyquist plot $\eta(\omega_n, \Phi)$ approaches a 45° slope in the fourth quadrant, which corresponds to a plot of the form $\eta(\omega_n, \Phi) \approx (i\omega_n)^{-1/2}$. This behavior can be easily derived by analyzing the reaction-free case $\Phi = 0$. For $\Phi = 0$, one has that $\eta(\omega_n, 0) = \tanh[(i\omega_n)^{1/2}]/(i\omega_n)^{1/2}$. One can show that $\tanh[(i\omega_N)^{1/2}] \approx 1$ holds at high-frequency conditions, which leads to the approximation $\eta(\omega_N, \Phi) \approx (i\omega_N)^{-1/2}$. Thus the high-frequency behavior $\eta(\omega_N, \Phi) \approx (i\omega_N)^{-1/2}$ corresponds to a regime controlled by the diffusion mechanism.

Summing up, the better performance for the reaction–diffusion process (Eqs. 8 and 9) is found for steady-state (that is, zero frequency) operating conditions. Besides, two regimes separated by the characteristic diffusion frequency ω_d are observed in the behavior of the DEF $\eta(\omega_n, \Phi)$:

(1) A low-frequency regime where the performance of the

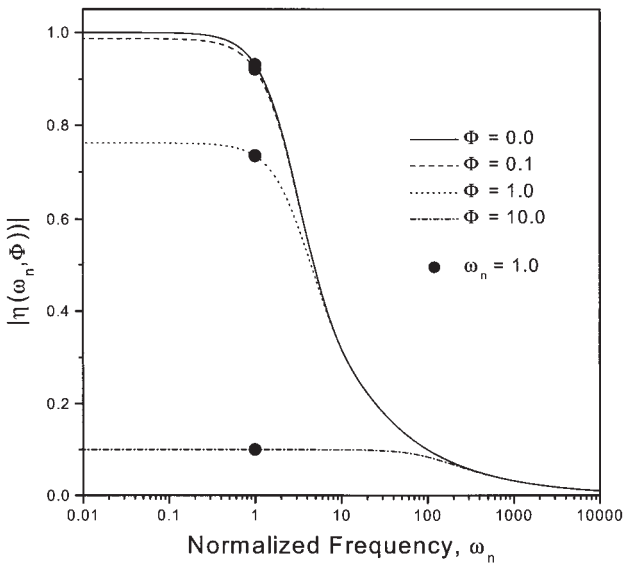

Figure 2. Magnitude Bode plot corresponding to the conditions of Figure 1.

Notice that $|\eta(\omega_n, \Phi)|$ is a decreasing function of the frequency ω_n.

reaction–diffusion process is not seriously deteriorated. Disturbances with frequency components in the range $\omega < \omega_d$ do not have a significant effect on the supply of molecules to the reaction mechanism.

(2) A high-frequency regime where the performance is seriously depleted. Because of high-frequency perturbations, the molecules are unable to penetrate the particle, such that the reaction rate dynamic $R(s_n)$ is seriously affected.

It is noticed that for the low-frequency regime $|\eta(\omega_n, \Phi)| \approx \bar{\eta}(\Phi)$. That is, the DEF is almost equal to the nondynamic EF. This shows that for long times (corresponding to $\omega_n \to 0$) or for low-frequency perturbations one can take the quasi-steady-state model $R(t) = \bar{\eta}(\Phi)Vkc_b(t)$ to compute the reaction rate behavior $R(t)$. Indeed, this is an assumption commonly made in practice.

Low-Order Dynamic Modeling Based on DEF

From the interpretation of the DEF as a linear operator between reaction rates, by considering that $R_b(s_n) = kVC_b(s_n)$, the exact dynamics of the particle reaction rate $R(s_n)$, in terms of boundary concentration dynamics $C_b(s_n)$, are described in the Laplace domain as follows:

$$R(s_n) = g(s_n, \Phi)C_b(s_n) \tag{17}$$

where

$$g(s_n, \Phi) \overset{def}{=} kV\eta(s_n, \Phi)$$

Equation 17 describes the dynamics $R(s_n)$ affected by the boundary concentration dynamics $C_b(s_n)$. Because the operator $g(s_n, \Phi)$ is causal, there exist matrices (A, B, C) such that the dynamics of Eq. 17 can be described in state-space form. That is, if z is a state vector, it is possible to write[10]

$$\frac{dz(t_n)}{dt_n} = Az(t_n) + Bc_b(t_n)$$
$$R(t_n) = Cz(t_n) \tag{18}$$

where, given that $s_n = s\omega_d$, $t_n = t\omega_d = tD/L^2$ is a dimensionless time variable. One has that the equality $g(s_n, \Phi) = C(s_nI - A)^{-1}B$ must be satisfied. Unfortunately, the order of the DEF operator is *infinite*, implying that the state vector z is infinite-dimensional. To see that the order of $\eta(s_n, \Phi)$ is infinite, let us look at the simplest rectangular geometry case: $\eta(s_n, \Phi) = \tanh[\Psi(s_n)]/\Psi(s_n)$. In terms of fundamental exponentials, the operator $\eta(s_n, \Phi)$ can be written as

$$\eta(s_n, \Phi) = \frac{(e^{\sqrt{\Phi^2+s_n}} - e^{-\sqrt{\Phi^2+s_n}})}{\sqrt{\Phi^2 + s_n}\,(e^{\sqrt{\Phi^2+s_n}} + e^{-\sqrt{\Phi^2+s_n}})} \tag{19}$$

The order of the operator $\eta(s_n, \Phi)$ is equal to the number of roots of the characteristic equation

$$E(s_n, \Phi) = \sqrt{\Phi^2 + s_n}\,(e^{\sqrt{\Phi^2+s_n}} + e^{-\sqrt{\Phi^2+s_n}})$$

One observes that a single root is located at Φ^2. However, because the equation is transcendental, the part $e^{-\sqrt{\Phi^2+s_n}} + e^{\sqrt{\Phi^2+s_n}}$ contains infinitely many (complex) roots. This property recovers, in some cases, the fact that the reaction rate dynamics $R(t)$ depends on a distributed reaction–diffusion mechanism.

The above result shows that, although for the steady-state case the EF concept leads to a simple model for the reaction rate $\bar{R}$, for the dynamic case such a concept leads to an infinite-dimensional model that is as sophisticated as the original one given by the partial differential equation (Eq. 8). However, an advantage of the DEF-based model $R(s_n) = g(s_n, \Phi)C_b(s_n)$, compared to the original one given by Eq. 8, is that the dependency on the spatial variable x has been removed. In fact, the transfer function $g(s_n, \Phi) = kV\eta(s_n, \Phi)$ depends only on the temporal operator $s_nc = \partial c/\partial t$. We will exploit this characteristic to approximate the infinite-dimensional model $R(s_n) = g(s_n, \Phi)C_b(s_n)$ by a simpler finite-dimensional one, $R(s_n) \cong h(s_n, \Phi)C_b(s_n)$, where $h(s_n, \Phi)$ denotes a finite-dimensional transfer-function approximating the infinite-dimensional one, $g(s_n, \Phi)$.

The magnitude Bode plot of the DEF (see Figure 2) shows that the transfer function $g(s_n, \Phi)$ behaves as a low-pass filter. In this form, the type of parabolic PDE systems given by Eqs. 8 and 9 is characterized by a few dominant modes that can capture the dominant long-term spatiotemporal behavior of the concentration equation. This suggests that the infinite-dimensional dynamics of the reaction rate $R(s)$ can be adequately approximated with a finite-dimensional low-order model. As mentioned earlier, this is equivalent to finding a rational transfer function $h(s_n, \Phi)$ approximating the infinite-dimensional one, $g(s_n, \Phi)$. In the following, we will explore the use of simple first-order and second-order models to approximate the reaction rate dynamics.

The idea of exploiting the existence of dominant modes for computing (finite-dimensional) models for reaction–diffusion equations is not new. Methods based on a singular perturbation formulation by Galerkin's method have led to an accurate description of reaction-rate dynamics. In turn, such low-order approximations have allowed successful application to the control of distributed processes.[6,8,9] The distinctive feature of our approach is that it relies on an approximation of a transfer function that, as done in this work, can be made with classical frequency response tools.

First-Order Approximate Model

A first-order transfer function is surely the simplest approximate model for the reaction dynamics. Similar approximate modeling for the average concentration was previously proposed by Szukiewicz.[4] The Bode plot of the dynamic effectiveness factor (see Figure 2) shows that the magnitude $|\eta(\omega_n, \Phi)|$ is a monotonous decreasing function with limits $|\eta(0, \Phi)| \to \bar{\eta}(\Phi)$ as $\omega \to 0$ and $|\eta(\omega_n, \Phi)| \to 0$ as $\omega \to \infty$. This suggests the following stable first-order model structure:

$$h(s_n, \Phi) = \frac{\alpha(\Phi)}{\tau_n(\Phi)s_n + 1}$$

where $\alpha(\Phi)$ is a steady-state gain and $\tau_n(\Phi)$ is a (normalized) time constant. Given that $R(s_n) \cong h(s_n, \Phi)C_b(s_n)$ and $h(0, \Phi) =$

$\alpha(\Phi)$, one has $\bar{R} = \alpha(\Phi)\bar{c}_b$ for steady-state conditions. To retain the steady-state characteristic of the exact dynamics $R(s_n) = g(s_n, \Phi)C_b(s_n)$, the equality

$$\alpha(\Phi) = kV\bar{\eta}(\Phi) \tag{20}$$

should hold, which leads to the approximate model

$$h(s_n, \Phi) = \frac{kV\bar{\eta}(\Phi)}{\tau_n(\Phi)s_n + 1} \tag{21}$$

Interestingly, by recalling that $g(s_n, \Phi) = kV\eta(s_n, \Phi)$, the approximation problem $h(s_n, \Phi) \approx g(s_n, \Phi)$ is equivalent to finding a first-order approximation of the form $\bar{\eta}(\Phi)/[\tau_n(\Phi)s_n + 1]$ to the exact DEF $\eta(\omega_n, \Phi)$. That is,

$$\eta(\omega_n, \Phi) \approx \frac{\bar{\eta}(\Phi)}{\tau_n(\Phi)s_n + 1} \tag{22}$$

Given the linearity of the approximate model, without losing generality one can assume that $R(t_n = 0) = 0$. In fact, these initial condition is the steady-state value $R = 0$ corresponding to the input $c_b \equiv 0$. In this way, under the aforementioned initial condition assumption, the output $R(t_n)$ can be seen as a deviation variable from the steady-state value $R \equiv 0$. In this way, a time-domain realization of the approximate first-order model for the particle reaction rate dynamics is

$$\frac{dR(t_n)}{dt_n} = \tau_n(\Phi)^{-1}[Vk\bar{\eta}(\Phi)c_b(t_n) - R(t_n)] \tag{23}$$

Notice that, for $c_b(t_n) = \bar{c}_b$, $R(t_n) \rightarrow Vk\bar{\eta}(\Phi)\bar{c}_b$ asymptotically.

The frequency domain (that is, $s_n \rightarrow i\omega_n$) is used to compute the time constant in Eq. 22 according to the following procedure:

(1) Decompose the complex function $\eta(\omega_n, \Phi)$ into its real (Re) and imaginary (Im) parts as follows:

$$\eta(\omega_n, \Phi) = \mathrm{Re}[\eta(\omega_n, \Phi)] + i\,\mathrm{Im}[\eta(\omega_n, \Phi)] \tag{24}$$

(2) For convenience in notation, let

$$f(\omega_n, \Phi) \overset{def}{=} \frac{\bar{\eta}(\Phi)}{\tau_n(\Phi)i\omega_n + 1}$$

This function can be written in terms of its real and imaginary parts as follows:

$$f(\omega_n, \Phi) = \left[\frac{\bar{\eta}(\Phi)}{\tau_n(\Phi)^2\omega_n^2 + 1}\right] + i\left[\frac{-\bar{\eta}(\Phi)\tau_n(\Phi)\omega_n}{\tau_n(\Phi)^2\omega_n^2 + 1}\right] \tag{25}$$

(3) Pose an approximate model-matching problem to compute the time constant $\tau_n(\Phi)$. By matching the real and imaginary parts of $f(\omega_n, \Phi)$ and $\eta(\omega_n, \Phi)$ (see Eqs. 24 and 25), the following two approximation problems should be solved:

$$\mathrm{Re}[\eta(\omega_n, \Phi)] \approx \frac{\bar{\eta}(\Phi)}{\tau_n(\Phi)^2\omega_n^2 + 1} \tag{26}$$

and

$$\mathrm{Im}[\eta(\omega_n, \Phi)] \approx \frac{-\bar{\eta}(\Phi)\tau_n(\Phi)\omega_n}{\tau_n(\Phi)^2\omega_n^2 + 1} \tag{27}$$

It has been established that the complex function $\eta(\omega_n, \Phi)$ is infinite-dimensional, whereas $f(\omega_n, \Phi)$ is only one-dimensional. In general, an exact solution to the model-matching problem $f(\omega_n, \Phi) = \eta(\omega_n, \Phi)$ does not exist. Thus an approximate model-matching problem should be posed instead. Because the model-matching problems expressed in Eqs. 26 and 27 cannot be solved for the whole frequency range, model matching can be satisfied only for a limited frequency range. It is suggested to pose the approximate model-matching problems in a frequency range around the steady-state condition $\omega_n = 0$. In fact, given that the steady-state equality $f(0, \Phi) = \eta(0, \Phi) = \bar{\eta}(\Phi)$ was forced to hold, extending the matching to frequencies sufficiently close to $\omega_n = 0$ will guarantee the asymptotic convergence $R(t) \rightarrow Vk\bar{\eta}(\Phi)c_b$.

(4) Compute a zeroth-order Taylor expansion of both sides of Eq. 26 at steady-state conditions. Such expansion gives $\mathrm{Re}[\eta(0, \Phi)] \approx \bar{\eta}(\Phi)$, which is an outcome of Eq. 20.

(5) Compute a first-order Taylor expansion of both sides of Eq. 27 at steady-state conditions. Taking note that $\mathrm{Im}[\eta(0, \Phi)] = 0$, one then obtains the following relationship:

$$\mathrm{Im}[\eta(0, \Phi)]'\omega_n \approx -\bar{\eta}(\Phi)\tau_n(\Phi)\omega_n$$

where $\mathrm{Im}[\eta(0, \Phi)]'$ is the derivative of $\mathrm{Im}[\eta(0, \Phi)]$ with respect to the frequency ω_n. By assuming the equality $\mathrm{Im}[\eta(0, \Phi)]'\omega_n = -\bar{\eta}(\Phi)\tau_n(\Phi)\omega_n$, an estimate of the time constant is given by

$$\tau_n(\Phi) = -\frac{\mathrm{Im}[\eta(0, \Phi)]'}{\bar{\eta}(\Phi)} \tag{28}$$

Figure 3 shows that the derivative $\mathrm{Im}[\eta(0, \Phi)]' < 0$ for Φ, which implies that the time constant given by Eq. 28 is well defined [that is, $\tau_n(\Phi) > 0$].

(6) Because $\eta(\omega_n, \Phi)$ is a sophisticated function, the attempt to analytically obtain $\mathrm{Re}[\eta(\omega_n, \Phi)]$ and $\mathrm{Im}[\eta(\omega_n, \Phi)]$ is not possible in general. Instead, numerical methods can be used to compute the time-constant estimate as specified by Eq. 28. Specifically, for a given Thiele modulus, the imaginary part as a function of frequency is computed by a numerical routine. This can be made with standard FORTRAN or MATLAB® packages. Next, the derivative $\mathrm{Im}[\eta(0, \Phi)]'$ is approximated as a forward finite difference:

$$\mathrm{Im}[\eta(0, \Phi)]' \simeq \frac{\mathrm{Im}[\eta(\delta, \Phi)] - \mathrm{Im}[\eta(0, \Phi)]}{\delta}$$

for a sufficiently small $\delta > 0$. Our experience has shown that $\delta = 10^{-2}$ suffices to obtain a stable finite-difference approxi-

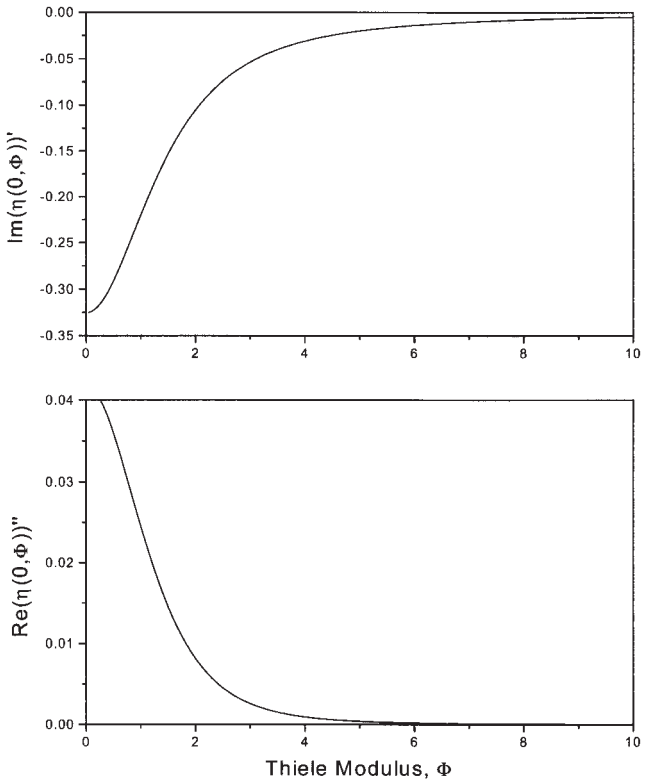

Figure 3. Derivatives Re[$\eta(0, \Phi)$]″ and Im[$\eta(0, \Phi)$]′ of the DEF $\eta(\omega_n, \Phi)$ around steady-state condition $\omega_n = 0$.

mation. Finally, an estimate of the time constant is computed with Eq. 28.

Figure 4 describes the function $\tau_n(\Phi)$ given by Eq. 28. Observe that $\tau_n(\Phi)$ is a monotonous decreasing function. That is, the faster the chemical reaction, the faster the reaction rate dynamics of the catalyst particle. The slower dynamics corresponds to a purely diffusional process with limiting (normalized) time constant $\tau_n(0) = 1/3$. Figure 5 shows the magnitudes of the exact DEF $\eta(\omega_n, \Phi)$ and the approximate first-order $\bar{\eta}(\Phi)/[\tau_n(\Phi)\omega_n + 1]$ complex functions. Acceptable approximation is observed for normalized frequencies $< \omega_n$, which corresponds to frequencies below the diffusion characteristic frequency ω_d. Some deviations are observed in the high-frequency range. It is also observed that the smaller the Thiele modulus, the better the first-order approximation. This is because for a small Thiele modulus, the whole catalyst space is penetrated by diffusion molecules, yielding a uniform particle reaction rate dynamics.

Second-Order Approximate Model

Second-order models can also be used, which are still simple approximate models that do not introduce a serious increment in the computational complexity. Assume a stable second-order model parameterized as follows:

$$h(s_n, \Phi) = \frac{Vk\bar{\eta}(\Phi)}{\tau_n(\Phi)^2 s_n^2 + 2\tau_n(\Phi)\xi(\Phi)s_n + 1} \tag{29}$$

where $\xi(\Phi) > 0$ is a damping factor. Similar to the first-order case, a time-domain realization of the approximate second-order model is

$$\tau_n(\Phi)^2 \frac{d^2R(t_n)}{dt_n^2} + 2\tau_n(\Phi)\xi(\Phi)\frac{dR(t_n)}{dt_n} + R(t_n) = Vk\bar{\eta}(\Phi) \tag{30}$$

Because $\tau_n(\Phi)^2 s_n^2 + 2\tau_n(\Phi)\xi(\Phi)s_n + 1$ is a stable polynomial, one has that, for $c_b(t) = \bar{c}_b$, $R(t_n) \rightarrow Vk\bar{\eta}(\Phi)\bar{c}_b$ asymptotically.

Similar steps that led to an expression for the time constant for the first-order model can be followed to estimate the model parameters $\tau_n(\Phi)$ and $\xi(\Phi)$. The corresponding steps are the following:

(1) Same step as in the first-order model case.

(2) In this case,

$$f(\omega_n, \Phi) = \frac{\bar{\eta}(\Phi)}{[1 - \tau_n(\Phi)^2\omega_n^2] + i[2\tau_n(\Phi)\xi(\Phi)\omega_n]} \tag{31}$$

which, when decomposed into its real and imaginary parts, yields

$$f(\omega_n, \Phi) = \left[\frac{1 - \tau_n(\Phi)^2\omega_n^2}{\gamma(\omega_n, \Phi)}\right] + i\left[\frac{-2\tau_n(\Phi)\xi(\Phi)\omega_n}{\gamma(\omega_n, \Phi)}\right] \tag{32}$$

where $\gamma(\omega_n, \Phi) = [1 - \tau_n(\Phi)^2\omega_n^2] + [2\tau_n(\Phi)\xi(\Phi)\omega_n]^2$.

(3) The model-matching problems are obtained as follows:

$$\mathrm{Re}[\eta(\omega_n, \Phi)] \approx \frac{1 - \tau_n(\Phi)^2\omega_n^2}{\gamma(\omega_n, \Phi)} \tag{33}$$

and

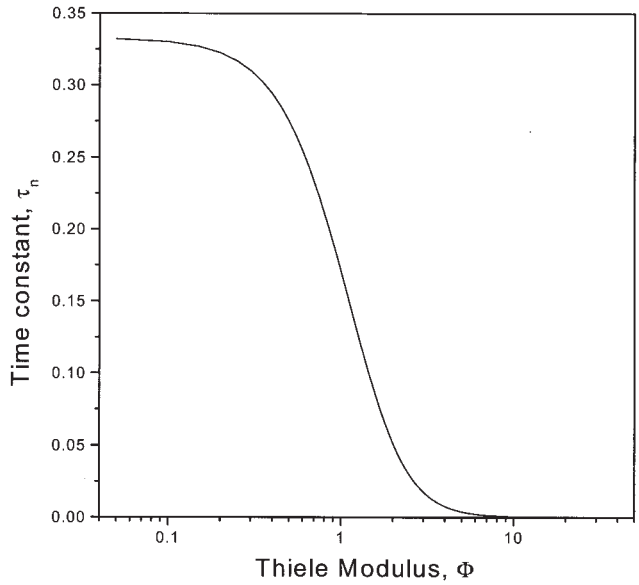

Figure 4. Estimated time constant for a first-order model from a model matching problem around steady-state condition.

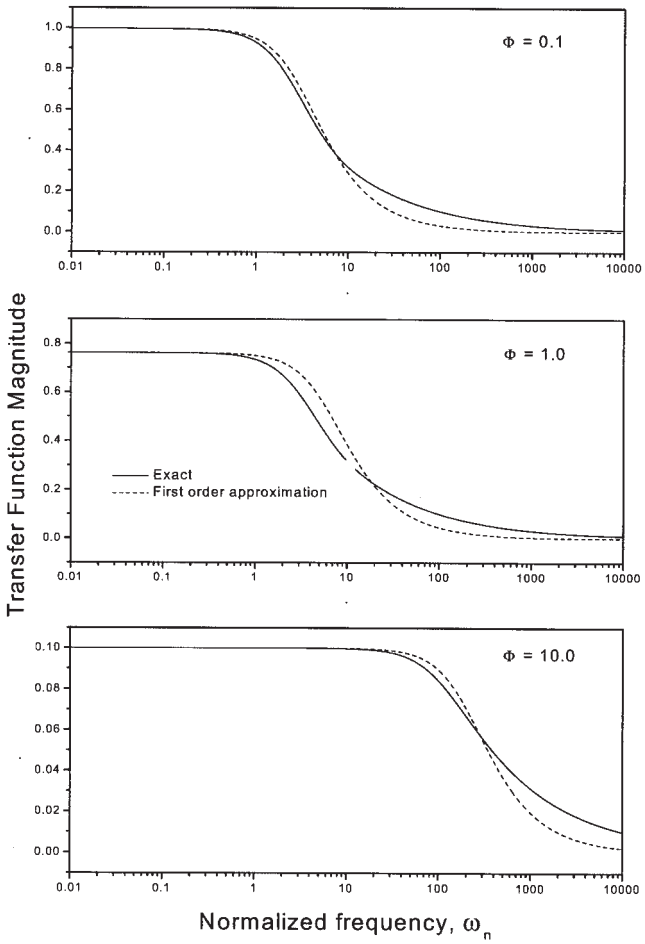

Figure 5. Actual $\eta(s_n, \Phi)$ and approximate first-order $\{[\bar{\eta}(\Phi)]/[\tau_n(\Phi)s_n + 1]\}$ dynamic EF.

$$\mathrm{Im}[\eta(\omega_n, \Phi)] \approx \frac{-2\tau_n(\Phi)\xi(\Phi)\omega_n}{\gamma(\omega_n, \Phi)} \tag{34}$$

(4) A second-order Taylor expansion of Eq. 33 around steady-state condition $\omega_n = 0$ is computed. In Figure 3 one can observe that $\mathrm{Re}[\eta(0, \Phi)]' = 0$, which yields the approximation

$$\bar{\eta}(\Phi) + \frac{1}{2}\mathrm{Re}[\eta(0, \Phi)]''\omega_n^2 \approx \bar{\eta}(\Phi) - 2\tau_n(\Phi)^2\omega_n^2 \tag{35}$$

In this way, by matching second-order frequency power, the following time-constant estimate is obtained:

$$\tau_n(\Phi) = \sqrt{-\frac{1}{4}\mathrm{Re}[\eta(0, \Phi)]''} \tag{36}$$

Figure 3 shows that the second derivative $\mathrm{Re}[\eta(0, \Phi)]'' > 0$. This implies that $\tau_n(\Phi)$ as given by Eq. 36 is not well defined.

The above analysis is interesting as it shows the impossibility of computing a time constant for a stable second-order model around steady state conditions. Although the parameter of the second-order model Eq. 31 can be estimated by means of other (*e.g.*, optimization-based) methods, it was shown that a matched second-order model around steady-state conditions for the reaction–diffusion process does not exist.

Extension to the nonlinear case

In this work, we have considered reaction–diffusion processes with linear reaction rates. This allowed a model-reduction methodology based on a transfer function; that is, the effectiveness factor in dynamic conditions. Although by itself the DEF concept introduced in the preceding sections can be of interest to researchers working in reaction engineering, the model-reduction problem for linear reaction rates is rarely of practical importance for such applications as process control. In fact, it is very likely that the reaction rates are nonlinear in real processes. As described earlier, the model-reduction technique based on frequency-response tools cannot be used for reaction–diffusion processes with nonlinear reaction rates because a transfer function cannot be computed (only *local* transfer functions can be computed). To overcome this problem, Szukiewicz[11] proposed to linearly approximate the reaction rate and compute a first-order model reduction based on such approximation. By using heuristic arguments, the nonlinear nature of the reaction–diffusion processes is subsequently recovered. A drawback of Szukiewicz's proposal is its lack of a systematic procedure to evaluate the model-reduction error. Moreover, high-order extensions to improve the approximation are not reported.

Well-established model-reduction methods (for example, Galerkin) for reaction–diffusion equations are based on the following observation. The concentration dynamics is driven by diffusion mechanisms modeled as $D\Delta c$, and the reaction activity is described, in general, by a nonlinear function $f(c)$. The latter is a pointwise function, and so it does not introduce "spatial memory." The former, given its distributed nature, involves an infinite-dimensional operator, which introduces an infinite number of dynamic modes. Thus, a procedure aimed at obtaining a finite-dimensional model should focus on the approximation of the diffusion operator. This idea has found sound applications in the computation of finite-dimensional controllers for the reaction–diffusion processes by Galerkin methods.[6,8,9] Given the *linear* nature of the diffusion operator, the same idea can be exploited to obtain reduced-order models by classical response-frequency tools. The rationale behind this proposal is that, as in Galerkin methods, a reduced-order model retains the dominant modes of the diffusion operator.

In this way, a first-order model contains an estimate of the dominant time constant of the process dynamics that, for many process applications, suffices to compute an industrial [such as proportional integral (PI)] feedback controller.[12]

To illustrate these ideas in a preliminary way, consider a reaction–diffusion process with a nonlinear reaction rate

$$\frac{\partial c}{\partial t} = D\Delta c - f(c)$$

with Dirichlet-type boundary conditions (see Eq. 9). In the spirit of the Galerkin method, let us compute an approximation to the distributed part of the above equation. To this end, given the pointwise nature of $f(c)$, consider the reactionless equation $\partial c/\partial t = D\Delta c$ and compute the corresponding transfer function

as done above. This is equivalent to taking $\eta(s_n, 0)$. Subsequently, compute a first-order approximation to give $\bar{\eta}(0) = 1$ and $\tau_n(0) \cong 1/3$ (see Figure 4). This implies that the dominant time constant for the diffusion operator (in rectangular coordinates) is equal to 1/3. By reincorporating the nonlinear reaction rate evaluated at average concentration conditions, the approximate first-order model for the average concentration dynamics $\bar{c}$ can be written as

$$\frac{d\bar{c}}{dt} = \frac{3D}{R_p}[c_b(t) - \bar{c}] - f(\bar{c})$$

where $c_b(t)$ is the boundary concentration and R_p is the particle radius. It is interesting to remark that for spherical coordinates the dominant time constant is $\tau_n(0) \cong 1/15$, which recovers the result reported by Szukiewicz.[11] One advantage of the approach described above is that high-order approximations can be obtained by increasing the approximation order of the transfer function $\eta(s_n,0)$. In such a case, the models can be expressed as in the following:

$$\frac{d\bar{c}}{dt} = \xi(t) - f(\bar{c})$$

where $\xi(t)$ is the output of a linear system and $\xi(s) = h(s)c_b(s)$, and $h(s)$ is a rational approximation to the transfer function $h(s) : c_b(s) \rightarrow \bar{c}(s)$ corresponding to the reactionless diffusion system.

It is interesting to note that when the method described above is used in the *linear* case, the approximate dynamics are given by

$$\frac{d\bar{c}}{dt} = 3[c_b(t) - \bar{c}] - \Phi^2\bar{c}$$

In this way, the estimated time constant is $\tilde{\tau}_n(\Phi) = (3 + \Phi^2)^{-1}$. As $\Phi \rightarrow 0$, one obtains $\tilde{\tau}_n(0) = 1/3$. Figure 6 compares this simple approximation with that obtained with the more formal method of the preceding section (see Figure 4). For all Thiele moduli, the simple expression $\tilde{\tau}_n(\Phi)$ yields larger time-constant values. Because the time constant shown in Figure 4 was computed from a matching problem around *steady-state conditions*, such a result could be expected, given that a smaller time-constant value leads to faster dynamics convergence to steady-state conditions. In fact, the approximation $\tilde{\tau}_n(\Phi)$ does not take in account the effects of the reaction dynamics on the diffusion dynamics. For completeness, Figure 6 also shows the estimated time constant from Szukiewicz's methodology. Observe that the result is quite similar to the result obtained in this work in that the former was also derived from a steady-state approximation problem. Perhaps the main advantage of the approach in this paper with respect to that of Szukiewicz is that a formal framework to compute reduced-order models is used, which allows an easier extension to more general situations (such as computation of high-order approximations).

Summing up, some possible extensions to the nonlinear case, of the model-reduction method described herein can be designed by following ideas from Galerkin's methods. Given that the main focus of this paper is on defining a DEF and its usage to obtain reduced-order models, the issue of computing reduced-order models for nonlinear kinetics should be explored in a subsequent work.

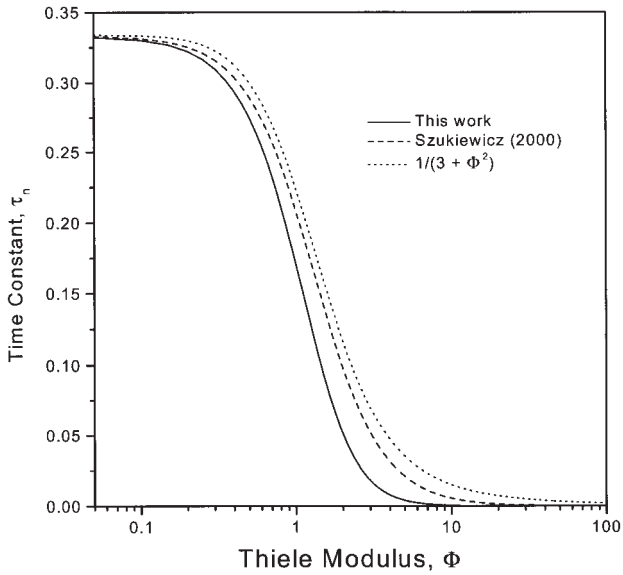

Figure 6. Comparison of the computed time constant from three different methods.

Simulations

This section is used to illustrate the performance of the model Eq. 23. For rectangular geometry, the dynamic reaction–diffusion problem can be written as

$$\frac{\partial c}{\partial t_n} = \frac{\partial^2 c}{\partial x^2} - \Phi^2 c \tag{37}$$

where $x \in [0, 1]$. The usual boundary conditions are

$$\begin{aligned} c(x, t_n) &= c_b(t_n) \qquad \text{for } x = 1 \\ \frac{\partial c(x, t_n)}{\partial x} &= 0 \qquad \text{for } x = 0 \end{aligned} \tag{38}$$

and the reaction rate provided by the catalyst particle is (see Eq. 7)

$$R(t_n) = Q\Phi^2 \int_0^1 c(x, t_n)dx \tag{39}$$

where Q is a constant flow rate. On the other hand, the corresponding first-order model (Eq. 23) can be written as (use the identification $k \rightarrow \Phi^2$)

$$\frac{dR(t_n)}{dt_n} = \tau_n(\Phi)^{-1}[Q\bar{\eta}(\Phi)\Phi^2 c_b(t_n) - R(t_n)] \tag{40}$$

Given the dimensionless description of Eqs. 37–40, only the Thiele modulus has to be specified. Because both the exact and

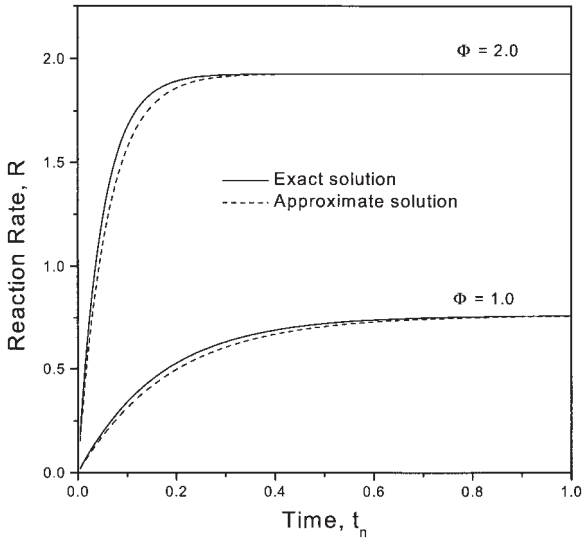

Figure 7. Step response for unit step of the exact and the approximate solutions for two different values of the Thiele modulus.

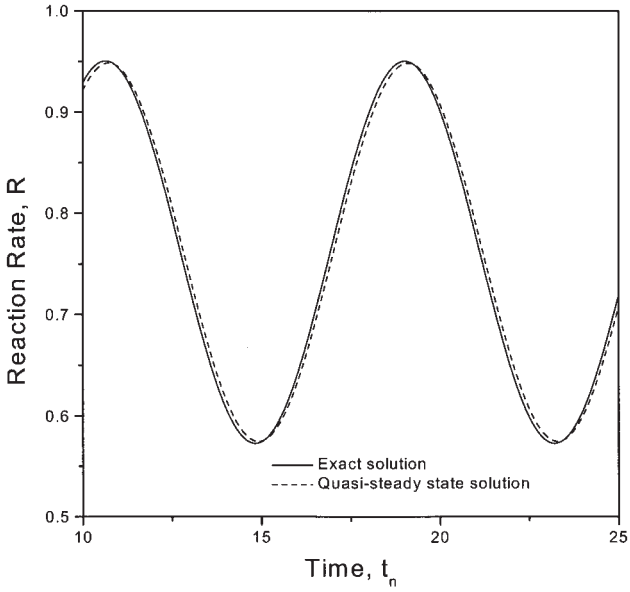

Figure 9. Exact and quasi-steady-state solutions for $\Phi = 1.0$ and $\omega_n = 0.75$.

the approximate models are linear, analytical solutions can be obtained, although such solutions are input dependent. That is, the analytical solution depends on the type of input (such as steps, ramps, etc.) considered. For the sake of simplicity in computations, we have used numerical methods to evaluate the system response in the face of different inputs $c_b(t_n)$. Specifically, a finite-differences method with a mesh of size 200 was used to reduce the partial differential equation problem of Eqs. 37 and 38 to a set of initial-value problems, which was integrated with a Runge–Kutta 4/5 integration method. Simpson quadrature was used to evaluate the integral in Eq. 39. Finally, a numerical solution to Eq. 40 was obtained with a Runge–Kutta 4/5 integration method. For all simulations, the value $A = 1$ was used.

Figure 7 shows the step response of the exact and approximate solutions for a step change from $\bar{c}_b = 0$ to $\bar{c}_b = 1.0$ at $t = 0.0$. It is observed that the response of the exact solution is faster than the approximate one. This is because $\tau_n(\Phi)$ is an upper bound of the estimate of the dominant time constant of the process. In fact, the dynamics of the exact reaction–diffusion process contains infinitely many dynamical modes whose effects are not recovered by the simple first-order model. Figure 5 shows good agreement between the exact and approximate dynamics in the low-frequency range. This is reflected in the fact that, as time increases, the approximate solution is closer to the exact one, as shown in Figure 6.

For $\Phi = 1.0$, Figure 8 shows simulation results for an oscillatory surface concentration of the form $c_b(t) = 1.0 + 0.25 \sin(\omega t_n)$. As expected from the results shown in Figure 5, good agreement between the exact and the approximate solutions is found for frequencies below the characteristic diffusion frequency $\omega_{d,n} = 1.0$. In fact, for $\omega_n = 0.1$ and $\omega_n = 1.0$ small deviations are observed during the transient dynamics. However, larger derivations (about 5%) are displayed for $\omega_n = 10.0$, where the important discrepancies in the frequency response can be observed. In this form, the larger the oscillation frequency, the larger the approximation error. Similar results were found for other Thiele modulus values.

Finally, let us illustrate the fact that $\eta(\omega_n, \Phi) \approx \bar{\eta}(\Phi)$ for $\omega_n < \omega_{d,n} = 1.0$. As noted earlier, this property yields the quasi-steady-state consideration $R(t) \approx A\bar{\eta}(\Phi)\Phi^2 c_b(t_n)$. Figure 9 shows the good agreement between the exact and the approximate reaction rates for $\omega_n = 1.0$. The plateau in the frequency response of the DEF as shown in Figure 5 can be considered as a support to the quasi-steady-state assumption commonly made in practice for heterogeneous reactor models.

It should be mentioned that, given the closeness of the different estimated time constants in Figure 6, minor differ-

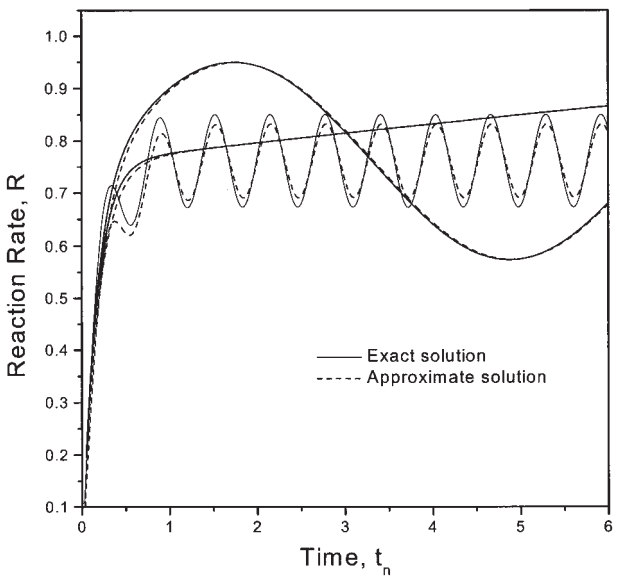

Figure 8. Frequency response of the exact and the approximate solution for $\Phi = 1.0$ and three different values of the oscillation frequency.

ences between the numerical results discussed above and numerical results from Szukiewicz's estimation were obtained. Such differences are found in the high-frequency (such as initial-conditions effect) regime.

Conclusions

In this paper, the problem of representing the distributed parameter dynamics of a catalyst particle by means of low-order (lumped parameter) models was addressed. As a preliminary step, an extension of the classical effectiveness factor (EF) concept to dynamic conditions was introduced. To do this, the EF was interpreted as an operator that transforms total reaction rates from surface to particle conditions. Based on this interpretation, a dynamic EF (DEF) was defined as a linear operator that transforms total reaction signals from surface to particle conditions. In this way, the DEF retains some information on the performance of a particle under dynamic perturbations. For common geometries, the computation of the DEF can be easily obtained from the nondynamic expression by a direct substitution of the classical Thiele modulus by a sort of "complex" Thiele modulus. The DEF results showed that the better catalyst performance is found at steady-state conditions; that is, dynamic perturbations deteriorate the catalyst particle effectiveness.

By departing from the DEF concept, a systematic method to obtain low-order models for the reaction dynamics was proposed. An algorithm to estimate the time constant for first-order models was proposed by using model-matching methods. The results showed that the larger the Thiele modulus, the smaller the time constant. Although our analysis showed that a stable second-order model cannot be computed from matching methods, more sophisticated second- and higher-order model structures should be explored in a future work. By following some approximation ideas from Szukiewicz,[11] extensions of the low-order model methodology to nonlinear reactions rate kinetics should be studied.

Literature Cited

1. Aris R. *The Mathematical Theory of Diffusion and Reaction in Permeable Catalysts*. Vol. 1. Oxford, UK: Clarendon Press; 1975.
2. Kim DH. Linear driving force formulas for diffusion and reaction in porous catalyst. *AIChE J.* 1989;35:343-346.
3. Goto M, Hirose T. Approximate rate equation for intraparticle diffusion with and without reaction. *Chem Eng Sci.* 1993;48:1912-1915.
4. Szukiewicz MK. New approximate model for diffusion and reaction in a porous catalyst. *AIChE J.* 2000;46:661-665.
5. Christofides PD, Daoutidis P. Feedback control of hyperbolic PDE systems. *AIChE J*. 1996;42:3063-3086.
6. Christofides PD, Daoutidis P. Finite-dimensional control of parabolic PDE systems using approximate inertial manifolds. *J Math Anal Appl*. 1997;216:398-420.
7. Sheng P, Zhou MY. Dynamic permeability in porous media. *Phys Rev Lett.* 1988;61:1591-1594.
8. Baker J, Christofides PD. Finite-dimensional approximation and control of nonlinear parabolic PDE systems. *Int J Contr*. 2000;73:439-456.
9. Christofides PD. *Nonlinear and Robust Control of Partial Differential Equation Systems: Methods and Applications to Transport-Reaction Processes*. Boston, MA: Birkhäuser; 2001.
10. Chen CT. *Introduction to Linear System Theory*. New York, NY: Holt, Rinehart & Winston; 1970.
11. Szukiewicz MK. An approximate model for diffusion and reaction in a porous pellet. *Chem Eng Sci.* 2002;57:1451-1457.
12. Morari M, Zafiriou E. *Robust Process Control.* New York, NY: Prentice-Hall; 1989.

Manuscript received Jan. 11, 2005, and revision received Apr. 4, 2005.